# scientific reports

OPEN

# Regarding the possible impact of forest fires on the radioactive pollution of groundwater in the chornobyl exclusion zone

Mykola Panasiuk[1], Mykhailo Buzynnyi[2✉], Serhii Kirieiev[3], Natalia Sosonna[1], Ihor Kovalenko[1] & Liubov Mykhailova[2]

Wood contamination in the Chornobyl Exclusion Zone (CEZ) with $^{137}$Cs and $^{90}$Sr reaches tens of kBq/kg. Fires are natural disasters that fundamentally alter the forest ecosystem. The largest fires in the CEZ occurred in 2020 at the temporary radioactive waste storage facility (PTLRW) known as "Red Forest", where the peak of $^{90}$Sr activity in wood was recorded. Subsequently, the level of $^{90}$Sr in groundwater samples from observation wells in this section of the CEZ increased by 2 to 60 times, rising from approximately 2 to about 180 Bq/l beginning in late 2022. The laboratory experiment utilized typical pinewood and forest litter samples. Laboratory studies show that burning 1 kg of dry pinewood produces approximately 2.8 g of ash, with a concentration of 90Sr in the ash that is approximately 360 times higher. The specific activity of $^{90}$Sr in the ash from six wood samples ranged from 160 to 3400 kBq/kg. Under suitable experimental conditions, the specific activity of $^{90}$Sr in the leachate samples ranged from 0.5 to 0.72 kBq/L. The proportion of $^{90}$Sr leached during the experiment varied from 12 to 33% for wood ash and 10.8–13.2% for forest litter ash. The complete combustion of 10% of the wood in the burn site area of the PTLRW "Red Forest" CEZ, influenced by a two-year rainfall volume, releases a secondary source of 90Sr available for migration with groundwater, with an intensity of at least 0.69 GBq/ha or more than 17 GBq/ha in the trench burial area of "Red Forest". Under these conditions, this source can reach 38 TBq in the 550 km² burn site area. The minerals in wood ash are easily washed away by water, leading to increased groundwater mineralization and higher ionic strength. This, in turn, reduces the soil's sorption capacity and enhances the migration capacity of $^{90}$Sr in the aquifer. The transformation of wood and forest litter into ash due to a forest fire concentrates radioactivity in it, which lies on the soil surface, making it vulnerable to rapid leaching by atmospheric precipitation. As a result, this radioactivity can become a significant local source of radioactive contamination of surface and groundwater, which requires updating the radioactivity monitoring regulations in the relevant observation wells of the CEZ.

**Keywords** Forest fires, Wood, Forest litter, Ash, Groundwater, $^{90}$Sr, Pollution sources, Mineralization, Ionic strength of the solution

Ash forms when wood burns, and the concentration of radionuclides in the ash increases significantly compared to the wood. This transformation raises radionuclide availability in ash for leaching through atmospheric precipitation and intense migration with water, including infiltration into groundwater. To analyze the problem, background information on the severity of wood and forest litter contamination, the characteristics of ash and the corresponding soil, the leaching of chemical elements from ash, and their effects on the properties of related water must be considered.

A study of the content and leachability of strontium (Sr) in ash from the combustion of household waste in domestic furnaces[1] showed that the most mobile fraction, which is washed out with water, ranges from 1.3% to almost 91% of the total Sr content. Meanwhile, the leachability of dry wood ash ranges from 11 to 18%.

[1]Institute for Safety Problems of Nuclear Power Plants, National Academy of Sciences of Ukraine, 36a Kirova Street, Chornobyl 07270, Ukraine. [2]State Institution O.M. Marzieiev Institute of Public Health of National Academy of Medical Sciences of Ukraine, 50, Hetman Pavlo Polubotko Str, Kyiv 02094, Ukraine. [3]State Specialized Enterprise Ecocentre, Vulytsya Shkil'na 4, Chornobyl 07270, Ukraine. ✉email: michael.buzynny@gmail.com

After a forest fire, a layer of ash and charred material quickly forms on the ground. This layer gradually diminishes and is redistributed by precipitation, wind, or animals through partial dissolution and incorporation into the soil. Ash can impact water runoff on the surface after a fire, depending on the properties of the ash and soil, as well as the thickness of the ash layer. The study's authors[2] focused significantly on the wettability of ash, which varies from low to extremely high and is determined by the burning temperature, depth, and organic carbon content. The interaction within the water-ash-soil system largely depends on soil properties.

The study's authors[3] argue that forest fire ash can pose significant risks to society due to the concentration of potentially harmful chemical components. After examining 148 samples (representing 42 types of ash), most exhibited an alkaline reaction, with a mean pH of 8.8 and a range of 6 to 11.2. The main components identified were organic carbon (mean value: 204 g/kg), calcium, aluminum, and iron (mean values: 47.9, 17.9, and 17.1 g/kg, respectively).

Based on ash samples from a pine forest fire in Portugal[4], the study determined that the ash filtrate had a higher pH and conductivity and was enriched in $Ca^{2+}$, $Mg^{2+}$, $Na^+$, $K^+$, and $Si^{4+}$ ions. Additionally, this study found that the solubility of potassium and calcium in charred residues was 1.7 times and 9.7 times higher, respectively, than in unburned forest litter.

The authors[5] investigated the impact of fire ash on water quality in the Gila River drainage in southwestern New Mexico, USA, over a five-year period. Following the introduction of fire ash, the water exhibited elevated concentrations of ammonium, nitrate, dissolved reactive phosphate (SRP), potassium, and alkalinity.

Increased mineralization raises groundwater's ionic strength. This diminishes soils' sorption properties, further contributing to enhanced radionuclide migration[6].

Studies of the forest conducted in Bavaria[7], where most of the $^{90}Sr$ is attributed to nuclear test fallout, demonstrated that the majority remains in the forest's organic horizons, indicating a very low migration rate for an extended period after the fallout.

A study of newly planted trees in the "Red Forest" area demonstrated significant contamination levels of $^{137}Cs$ and $^{90}Sr$, showing a notable individual contrast in their distribution across the tree trunk cross-Sect. [8]. The authors[9] made and calibrated a simulation model to depict the distribution of $^{90}Sr$ within components of the forest ecological system (*Pinus sylvestris L.*) based on findings from their recent experimental studies. According to the 2025 forecast derived from the model, wood contains 20%, while forest litter holds 14% of the total $^{90}Sr$ activity concentrated in the forest biosystem. Subsequent analyses of the wood from the "Red Forest," conducted between 2005 and 2018, indicated[10] that, despite a general decrease in the specific activity of $^{90}Sr$ across all compartments of the tree biomass, its total reserves in wood rose from 18 to 23 GBq/ha, respectively. Corresponding estimates derived from studies of trees planted in the trenches of the "Red Forest" wood burials reveal that $^{90}Sr$ reserves here have increased nearly sixfold, reaching approximately 560 GBq/ha, which constitutes about $(19 \pm 9)\%$ of the total reserve in the trench zone.

Therefore, recent fires in the Chornobyl NPP area have heightened the secondary redistribution of radioactivity and its transfer, resulting in additional surface and groundwater contamination. Fires are common due to the limited control over the forested areas of the Chornobyl Exclusion Zone. The largest fires (Fig. 1) occurred over an area of 554 km² in 2020[11,12]. It is known that fires accompanied the military occupation of the CEZ by Russian troops in 2022.

The authors[13] demonstrated that aerial emissions of $^{137}Cs$ and $^{90}Sr$ during burning experiments at the Chornobyl fire site reached up to 4.2% of the $^{137}Cs$ and 2.9% of the $^{90}Sr$ stocks. This suggests that most $^{137}Cs$ and $^{90}Sr$ remained in the charred residues on the ground after the fire. An analysis of results from a systematic study conducted in the fire-affected zone of the CEZ revealed that the water-soluble fractions of $^{137}Cs$ and $^{90}Sr$ in charred residues were significantly higher than those in the soil, which indicates their increased mobility[13]. The geometric means of the water-soluble and exchangeable forms of $^{137}Cs$ in the charred residues were 2.2% and 17.4%, respectively. The geometric means for the water-soluble and exchangeable forms of $^{90}Sr$ in the charred residues were 5.4% and 27.5%, respectively.

However, the extent of burnout of the charred residues used in this study is unknown. Therefore, the water-soluble fraction of $^{90}Sr$ content could be significantly higher for ashes with more complete burnout. However, no significant increase in the concentration of $^{137}Cs$ in the river catchment area of Chornobyl was observed after the forest fires. However, $^{90}Sr$ concentrations significantly increased, periodically exceeding the permissible levels for drinking water (2 Bq/l) in Ukraine[14]. The authors explain this increase by hydrologically driven transport processes of soluble $^{90}Sr$ from charred remains and the soil surface into the river during snowmelt and precipitation. They[13] stated that the fate of $^{137}Cs$ and $^{90}Sr$ in charred residues is currently unknown, but the dynamics of $^{137}Cs$ and $^{90}Sr$ in the environment are similar to those of K and Ca.

This study aimed to assess the secondary sources created after fires concerning $^{90}Sr$ migration with water, based on laboratory-measured properties of wood and forest litter ash samples, the corresponding activity concentrations of $^{137}Cs$ and $^{90}Sr$, and the extent of their leaching from wood and forest litter ash due to water corresponding to two years of rainfall. The activity concentrations of $^{137}Cs$ and $^{90}Sr$ in wood, forest litter, ash, and filtrate were measured to achieve this goal. The degree of $^{137}Cs$ and $^{90}Sr$ leaching from wood and forest litter ash was determined, and the dynamics of $^{90}Sr$ in groundwater samples from some wells located within the burnt areas of the "Red Forest" PTLRW site were analyzed.

## Materials and methods
### Wood and forest litter samples
For laboratory studies of wood ash and forest litter, we used the dry residue from samples collected in the Chornobyl Exclusion Zone in 1996, 2013, and 2021, which had been previously studied[15–17]. Wood samples (*Pinus sylvestris L.*) were taken at two sites near the Yaniv railway station. Forest litter samples were gathered near the Prypiat oil base, site 96/36. They correspond to characteristic morphological layers: A – a light upper layer

**Fig. 1**. Burns after the 2020 fires at the "Red Forest" PTLRW site.

of fresh litter, B – a thick layer with partial structural changes in the material, and C – a lower layer with severe decomposition. Given the long interval between wood samplings, we observed changes in the specific activity and ratio of radionuclides. Over time, the activity of $^{90}$Sr increased while $^{137}$Cs decreased, which is particularly significant in the most contaminated areas of the CEZ[8,10]. Wood samples I, II, and III were collected in 2013, while wood sample IV corresponded to one tree from 2021.

### Ashing of samples

Considering the ashing of wood and forest litter, we take into account general information related to sample concentration under heating — a safe temperature for $^{137}$Cs without losses is believed to be 450 °C. The appropriate temperature for $^{90}$Sr is 600 °C[18]. We also considered that burning biomass enriched with cesium in an open space resulted in a loss of cesium ranging from 40 to 70%, depending on temperature[19]. The review's authors[20] indicate that the magnitude of cesium emissions during laboratory combustion of contaminated biota depends on the temperature and design features of the experimental setup. As part of the laboratory experiment to obtain ash, we utilized the available equipment: a vertical muffle furnace and a stainless steel reaction vessel with a perforated lid for charring wood samples[15,17]. During the process, forced exhaust ventilation and a specialized chimney were used to cover the hot zone—the furnace opening with the top of the reactor vessel—and to carry the combustion products to the umbrella above, which limits their entry into the laboratory air. After the charring process was conducted with low oxygen for about an hour, we opened the lid of the reaction vessel, and the subsequent wood-burning process lasted an additional 16 to 20 h for the chopped wood sample.

Wood samples I, II, and III represented chopped wood, while wood sample IV represented chips. This determined the duration of the final combustion process, as the chips burned out more quickly. The temperature in both cases was 600ºC. Quantitative data on the ash preparation process are provided in Table 1. To control the variability of the process, sample I was repeated as I-A, and sample IV was prepared in three portions labeled IV-A, IV-B, and IV-C. The quality of the ash was assessed as satisfactory; visually, it appeared dark gray or had a brownish shade. The average ash content of wood (ash/dry material, $10^{-3}$) was $2.80 \pm 0.37$ ($N = 7$). The corresponding ash content coefficients ($10^{-3}$) for different layers of the forest litter were A – 29, B – 48, and C – 192, reflecting the increase in the proportion of the mineral fraction in the litter from the top (A) to bottom (C). The significant variation in ash content coefficients between samples of different litter layers allowed us to use them as they are without performing repeated samples. In addition, we estimated $^{137}$Cs losses during ashing as we did it and prepared additional ash samples of wood I-B, I-C, and I-D, see Table 2, with an average of $28 \pm 3\%$.

| Sample | Dry material, g | Ash, g | Ash/Dry×$10^{-3}$ | Dry/Ash | Ash code |
|---|---|---|---|---|---|
| | Wood | | | | |
| II | 360 | 0.98 | 2.72 | 367 | II |
| I | 360 | 0.89 | 2.47 | 404 | I |
| I-A | 360 | 0.84 | 2.32 | 428 | III |
| III | 360 | 1.11 | 3.08 | 324 | IV |
| IV A | 100 | 0.30 | 3.0 | 333 | V |
| IV B | 100 | 0.34 | 3.4 | 294 | VI |
| IV-C | 200 | 0.54 | 2.7 | 370 | VII |
| | | | 2.80 ± 0.37 | 360 ± 47 | |
| 96/36 | Forest litter | | | | |
| A | 33 | 0.9 | 29 | 37 | 96/36-A |
| B | 41 | 2.0 | 48 | 21 | 96/36-B |
| C | 25 | 4.8 | 192 | 5.2 | 96/36-C |

**Table 1**. Sample mass change while Ashing.

| Sample | Wood, g | Ash, g | $^{137}$Cs in wood, Bq | $^{137}$Cs in ash, Bq | Losses, % |
|---|---|---|---|---|---|
| I-B | 116 | 0.318 | 1.88 ± 0.15 | 1.22 ± 0.15 | 29% |
| I-C | 125 | 0.378 | 1.75 ± 0.15 | 1.32 ± 0.15 | 25% |
| I-D | 122 | 0.355 | 1.47 ± 0.15 | 1.01 ± 0.15 | 31% |
| | | | | | 28 ± 3% |

**Table 2**. Estimation of $^{137}$Cs losses while wood samples were converted to Ash at 600 °C.



**Fig. 2**. Syringe column (2 ml).

## Laboratory experiment on leaching $^{90}$Sr with water from Ash

In preparation for the laboratory experiment, 0.3 to 1.1 g of ash was obtained from the aforementioned wood samples. Disposable 2 ml and 5 ml medical syringes provided a compact and cost-effective experimental column (see Figs. 2 and 3), while successive portions of the filtrate were collected in 20 ml plastic vials.

**Fig. 3**. Syringe column (5 ml).

| N | Syringe volume | Inner diameter, mm | Syringe cross-sectional area, mm² | Sample mass, g | Conversion coefficient per m² | Ash mass per unit surface area, g/m² |
|---|---|---|---|---|---|---|
| 1 | 2 ml | 82 | 52.8 | 0.2154 | 18,940 | 4080 |
| 2 | 5 ml | 11.4 | 102.1 | 0.2154 | 9795 | 2110 |
| 3 | 5 ml | 11.4 | 102.1 | 0.105 | 9794 | 1028 |

**Table 3**. Ash loading parameters for different experimental conditions.

First experiment: 2 ml syringe (luer lock). For pre-wetting and subsequent filtration, an ash sample weighing about 0.2 g was placed between layers of cotton discs. The primary syringe containing the ash was positioned between two others to improve the structure and create additional water volume that could be loaded simultaneously. The lower syringe held extra filter material. Overnight, all the water filtered through the ash. The second portion of water was rejected because it stopped flowing through the syringe due to the excessively thick layer of ash.

The second experiment utilized a 5 ml syringe with an ash weight of about 0.2 g. A reinforced plastic tube with a specified diameter of 8 × 2.5 mm (Fig. 3) extended the column, which was positioned vertically in a stand.

Although passing water in five portions of 5 ml each was initially lengthy, over time, when the ash sample yielded, the increased portion to 20 ml caused no delay— the water flow was more intense. The planned volume of 125 ml of water was passed through within 3 to 4 h. Before the subsequent experiments, the ash loading per cross-sectional area of the experimental column was calculated (Table 3, rows 1 and 2). In option 2, the cross-sectional area was nearly doubled compared to option 1. Then, in option 3, the ash portion was reduced by half. Consequently, the column's cross-sectional area was approximately 1.0 cm², with the ash loading per cross-sectional area capped at about 1.0 kg/m².

Based on option 3, ash studies were conducted for sample I, where the water flow was faster than in option 2. The subsequent experiments for samples II and III were carried out simultaneously—all subsequent experiments adhered to option 3, utilizing 5 ml syringes and approximately 0.1 g of ash.

Since the task involved washing out a wide range of volumes, the first 5 ml portions were administered five times, followed by 20 ml portions also administered five times. After each experiment, ten filtrate samples were collected in separate vials. The first bottle in each set contained a slightly smaller volume because some water moistened the column material. Sampling data is provided in Table 4, which presents the cumulative volume of filtered water obtained for each step (vial). The volume (weight) of each portion of leachate was determined using precise laboratory digital scales with an uncertainty below 1%. The estimated uncertainty in measuring the $^{90}$Sr activity of corresponding individual consecutive samples is below 10%, and for sample S IV, it is below 15%. Individual weights and the $^{90}$Sr activity of filtrate samples were used to form the corresponding cumulative data presented in Table 4.

| Sample | N | 1 | 2 | 3 | 4 | 5 | 6 | 7 | 8 | 9 | 10 |
|---|---|---|---|---|---|---|---|---|---|---|---|
| | Wood samples | | | | | | | | | | |
| S II | *V, ml | 3.4 | 8.5 | 13.3 | 18.4 | 23.3 | 43.5 | 62.6 | 83.9 | 104.5 | 121.1 |
| | **A, Bq | 2.9 | 8.0 | 11.8 | 17.4 | 22.0 | 26.0 | 28.0 | 29.9 | 30.9 | 31.6 |
| S III | V, ml | 3.8 | 8.0 | 12.9 | 17.9 | 22.9 | 43.1 | 62.6 | 83.2 | 103.5 | 124.4 |
| | A, Bq | 2.7 | 7.4 | 12.6 | 14.4 | 15.1 | 17.0 | 17.8 | 18.4 | 18.9 | 19.4 |
| S IV | V, ml | 3.76 | 8.79 | 13.8 | 18.7 | 23.7 | 43.3 | 62.6 | 82.1 | 103.4 | 124.7 |
| | A, Bq | 0.6 | 1.0 | 1.4 | 1.5 | 1.7 | 2.3 | 2.9 | 3.4 | 3.8 | 4.2 |
| S V | V, ml | 3.8 | 8.8 | 13.7 | 18.7 | 23.7 | 45.1 | 64.2 | 84.1 | 102.9 | 123.2 |
| | A, Bq | 1.8 | 4.9 | 7.8 | 10.3 | 12.8 | 23.2 | 28.9 | 31.8 | 33.4 | 34.4 |
| S VI | V, ml | 3.8 | 8.8 | 13.7 | 18.7 | 23.7 | 45.1 | 64.2 | 84.1 | 102.9 | 123.2 |
| | A, Bq | 13.2 | 23.3 | 31.4 | 36.8 | 41.8 | 52.1 | 60.6 | 68.3 | 81.3 | 90.8 |
| S VII | V, ml | 3.3 | 8.5 | 12.9 | 17.9 | 22.9 | 43.0 | 64.0 | 84.4 | 104.0 | 121.4 |
| | A, Bq | 4.3 | 7.9 | 9.6 | 11.4 | 12.7 | 19.0 | 23.2 | 28.4 | 34.1 | 38.3 |
| | Forest litter, 96/36 | | | | | | | | | | |
| A | V, ml | 4.2 | 9.0 | 14.8 | 19.1 | 24.0 | 43.9 | 64.1 | 84.6 | 102.7 | 123.7 |
| | A, Bq | 1.3 | 2.3 | 3.0 | 3.5 | 3.9 | 4.8 | 5.5 | 6.0 | 6.3 | 6.8 |
| B | V, ml | 5.8 | 10.9 | 15.8 | 21.4 | 27.0 | 47.8 | 68.6 | 88.1 | 108.4 | 127.8 |
| | A, Bq | 2.2 | 3.6 | 4.9 | 6.1 | 7.0 | 9.1 | 10.5 | 11.1 | 11.8 | 12.3 |
| C | V, ml | 4.0 | 9.1 | 14.1 | 19.1 | 24.1 | 45.6 | 65.9 | 86.1 | 107.0 | 128.1 |
| | A, Bq | 15.7 | 30.3 | 36.8 | 40.5 | 43.3 | 50.8 | 54.9 | 58.9 | 61.2 | 64.0 |

**Table 4**. Cumulative data on leachate volume and the corresponding $^{90}$Sr activity for each studied wood and forest litter Ash with consecutive water samples, the uncertainty of leachate mass is below 1% when $^{90}$Sr activity– below 10% (for sample S IV – below 15%).

### Balance in the sample activity

Filtrate samples were prepared to measure the $^{90}$Sr content directly using a Quantulus 1220™ liquid scintillation spectrometer and the Cerenkov counting method to estimate the fraction of activity washed out of the sample due to the described experiment. To determine the residual $^{90}$Sr activity after the filtration procedure, the ash (wood) sample residues were dissolved by adding 1 M $HNO_3$. If necessary, a few drops of $H_2O_2$ were added to clarify the resulting solution.

### Measurement of $^{90}$Sr activity

The measurement scenario indicated that the activity of $^{90}$Sr significantly exceeded that of $^{137}$Cs. Based on a Quantulus 1220™ liquid scintillation spectrometer, the Cerenkov counting method accounts for the color quenching effect[21]. To standardize the volume in the first five portions of each set, the filtrate was diluted to 20 ml using distilled water. Measurements of the filtrates conducted immediately after the experiment revealed a low counting rate; however, subsequent measurements, even after a day, showed a rapid increase in the counting rate. This increase is attributed to the accumulation of $^{90}$Y, suggesting that primarily, only $^{90}$Sr was supplied with water. After two days, we could assess the results more effectively, considering the accumulation, and the final results were obtained later when the measurements were repeated after nearly two weeks, at which point $^{90}$Sr and $^{90}$Y were in equilibrium. The final estimate of $^{90}$Sr in the vial has an uncertainty of less than 10%.

The activity of $^{90}$Sr in residual ash samples from forest litter was evaluated using a solid-state beta spectrometer produced by Atom Komplex Prylad[22]. Due to the notable $^{90}$Sr activity, the measurement uncertainty stayed below 20%.

### Measurement of $^{137}$Cs activity

An ORTEC semiconductor spectrometer (MCB 918 + HPG detector GMX-25200) featuring a lead protective housing was utilized for measurements. The measurement of $^{137}$Cs content commenced with samples that, as anticipated, had the highest $^{137}$Cs activity, specifically the litter (layer C). Due to the limited sample volume and low $^{137}$Cs activity, it was necessary to study a combined cumulative sample. To accomplish this, 10 vials from each experiment were arranged in a 1-liter Marinelli vessel positioned in the lower part around the circumference. This method was justified because we were primarily interested in evaluating the total leaching of $^{137}$Cs. A certified Be-261 source and its derivatives were used for calibration ($^{137}$Cs).

### Results

Table 4 shows each sample vial's cumulative filtrate volume and $^{90}$Sr activity results. Table 5 presents the cumulative values of $^{90}$Sr and $^{137}$Cs activity, specifically the cumulative leaching activity over 10 steps, the residual $^{90}$Sr and $^{137}$Cs activity, and the balance of $^{90}$Sr and $^{137}$Cs activity within the samples, as well as the calculated percentage of leached activity. The fraction of leached $^{90}$Sr activity was calculated for each ash sample, whereas the leached $^{137}$Cs activity was measured in ash samples obtained from forest litter. In wood ash samples, the fraction of

| Sample, code | Ash code | Weight of ash, g (~) | Nuclide | Washed, Bq | Residue, Bq | Total, Bq | Washed up, % |
|---|---|---|---|---|---|---|---|
| Wood I | S-II | 0.2 | $^{90}$Sr | 31.6 | 104.0 | 135.6 | 23.3% |
| | | | $^{137}$Cs | 0.36 | < 0.05 | ≈ 0.36 | ≈ 89% |
| Wood I | S-III | 0.2 | $^{90}$Sr | 19.4 | 98.0 | 117.4 | 16.5% |
| | | | $^{137}$Cs | 0.41 | < 0.05 | ≈ 0.41 | ≈ 89% |
| Wood II | S-IV | 0.1 | $^{90}$Sr | 4.2 | 12.0 | 16.2 | 25.9% |
| | | | $^{137}$Cs | 0.37 | < 0.05 | ≈ 0.37 | ≈ 89% |
| Wood III | S-V | 0.1 | $^{90}$Sr | 34.4 | 70.0 | 104.4 | 33.0% |
| | | | $^{137}$Cs | 0.79 | < 0.05 | ≈ 0,79 | ≈ 89% |
| Wood IV | S-VI | 0.1 | $^{90}$Sr | 90.8 | 251.0 | 341.8 | 26.6% |
| | | | $^{137}$Cs | 1.59 | 0.2 | 1.79 | 89 ± 4% |
| Wood IV | S-VII | 0.1 | $^{90}$Sr | 38.3 | 280.0 | 318.3 | 12.0% |
| | | | $^{137}$Cs | 2.0 | 0.23 | 2.23 | 89 ± 3% |
| 96/36 A | A | 0.1 | $^{90}$Sr | 6.8 | 55.9 | 62.7 | 10.8% |
| | | | $^{137}$Cs | 2.8 | 5.2 | 8.0 | 35.0 ± 2.5% |
| 96/36 B | B | 0.1 | $^{90}$Sr | 12.3 | 78.8 | 91.8 | 13.5% |
| | | | $^{137}$Cs | 6.5 | 80 | 86.5 | 7.5 ± 1.5% |
| 6/36 C | C | 0.17 | $^{90}$Sr | 64.0 | 494 | 558 | 11.5% |
| | | | $^{137}$Cs | 8.0 | 715 | 723 | 1.1 ± 0.5% |

**Table 5.** Cumulative leaching balance ($^{90}$Sr vs. $^{137}$Cs) from Ash sample with water (V ≈ 125 ml), uncertainty of $^{90}$Sr activity is 10–15% when $^{137}$Cs – below 20% where applicable.

$^{137}$Cs activity was measured only in high-activity ash samples – S-VI and S-VII (89 ± 4%). The estimated leached fraction of $^{137}$Cs for other wood ash samples was also approximately 89%.

According to the data in Table 4; Fig. 4 (wood) and Fig. 5 (forest litter) show the cumulative $^{90}$Sr leaching with each portion of water for each ash sample studied.

The leaching rate of $^{137}$Cs was studied in just one sample set, specifically the litter and layer C, where the $^{137}$Cs content was measured for each of the 10 portions of water washed from a distinct portion of ash. It is similar to the $^{90}$Sr leaching rate, but near-complete saturation occurs during the initial five mL samples.

Using the data above, it can be concluded that burning wood and forest litter in the CEZ leads to ash becoming a significant secondary source of local environmental pollution, particularly affecting groundwater. According to estimates by[8], the reserves of $^{90}$Sr in wood outside the trenches containing buried radioactive waste in the PTLRW "Red Forest" area amounted to 23 GBq/ha. Even with the combustion (conversion to ash) of 10% of the wood and leaching from the ash, 30% of $^{90}$Sr per year becomes available for water migration. On each hectare of burned area, (23 GBq/ha ×0.1×0.3 = 0.69) 0.69 GBq/ha of $^{90}$Sr is available for migration with water. The corresponding fraction of $^{90}$Sr available for water migration over the entire burned area of 554 km² (55400 ha) in 2020[11,12] is (554 km² × 100 ha/km² × 0.69 GBq/ha = 38226) GBq, which is approximately 17 times higher than the $^{90}$Sr reserves in the water of the CNPP's cooling pond before its decommissioning – 2200 GBq[23]. Within the area of the burial trenches, the $^{90}$Sr reserves in wood reach 560 GBq/ha[8], which is nearly 25 times higher than in the surrounding territory. The estimates provided above are solely for pinewood ashes. When considering the recent $^{90}$Sr distribution forecast in the forest (*Pinus sylvestris L.*) ecosystem[7], refer to the introduction; forest litter constitutes a comparable portion, approximately 70%, compared to pinewood (14/20 = 0.7).

### Analysis of the dynamics of the $^{90}$Sr activity in the observation wells' water

Figure 6 (color) shows a map of the fire spread area since 2020 within a 10 km zone. This figure shows the lines of equal pressure and the direction of groundwater movement, indicated by red arrows. The movement of groundwater in the area of the fire at the Red Forest PTLRV is directed to the northeast. Wells K-2/1 and K-2/2 are located in the middle of the 2020 fire zone. Noticeable changes in the specific activity of $^{90}$Sr in groundwater were observed when analyzing the SSE Ecocentre routine monitoring data for observation wells K-2/1 and K-2/2, which are presented in Figs. 7 and 8. The corresponding tabular data are included in Supplementary Data Sets S.1 and S.2. In groundwater samples from well K-2/1, the $^{90}$Sr activity concentration increased from 15 to 98 Bq/l at the end of 2022, a 2–6 fold increase. In well K-2/2, in October 2022, the specific activity of $^{90}$Sr began to increase from 2.9 to 180 Bq/l, equivalent to a 10-60-fold increase (Fig. 8). Actually, the $^{90}$Sr increase in observation wells happened only 2.7 years after the fires.

The rise in $^{90}$Sr concentrations was likely caused by leaching with atmospheric precipitation that fell on ash and debris from wood and forest litter burned during the fire. Groundwater contamination occurs when atmospheric precipitation infiltrates the corresponding 3–4 m aeration zone's sandy soils. At the same time, the sorption properties of the soils can be significantly reduced because ashes contain high concentrations of $Ca^{2+}$, $Mg^{2+}$, $K^+$, and $Na^+$, which contribute to an increase in the migration capacity of $^{90}$Sr in the soils. The hypothesis regarding the effect of fires on groundwater contamination, observed in wells K-2/1 and K-2/2, is supported by the results of predictive simulation performed earlier under similar conditions[24].
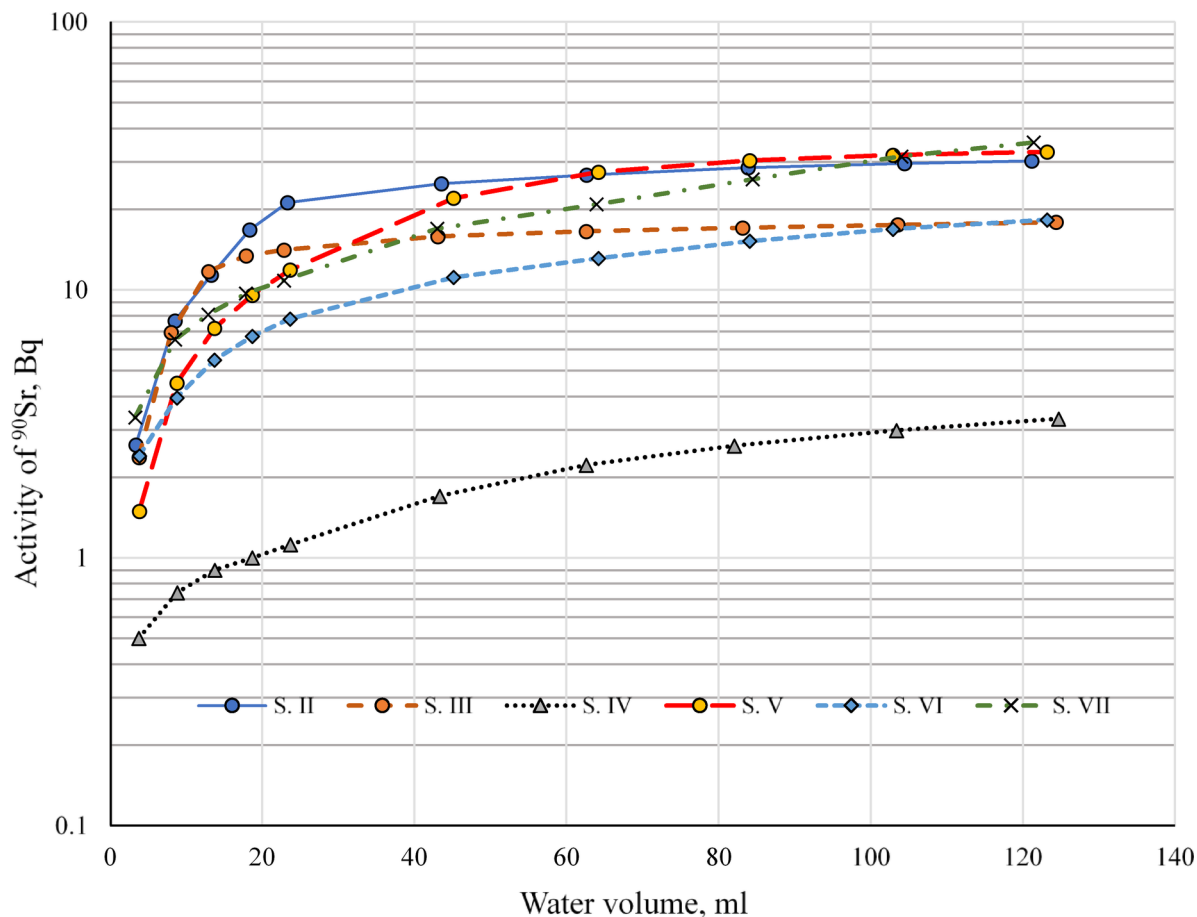
**Fig. 4**. Cumulative $^{90}$Sr activity leached from a pinewood ash sample with water, Bq.

The thickness of the aeration zone in the modeling was 2 m. The $^{90}$Sr inflow to the aquifer was modeled from the active surficial layer through the aeration zone. The distribution coefficient was determined at the level of 1 ml/h. According to modeling, the main predicted inflow of $^{90}$Sr to the groundwater level occurs after 200 days. Approximately 97% of the total inflow into the aquifer occurs within the 200–365 day time interval. In our case, the thickness of the aeration zone is 1.5 to 2.0 times greater. At the same time, the time taken for elevated concentrations of $^{90}$Sr to appear in water samples from observation wells is nearly three times greater.

Considering the difference in the thickness of the aeration zone, the assumption about the impact of fires on groundwater contamination observed in the wells, as mentioned above, seems realistic.

## Conclusions

Laboratory experiments demonstrated that burning 1 kg of pinewood from the Chornobyl zone ($N = 6$) results in an ash residue of $2.80 \pm 0.37$ g. This yields a $^{90}$Sr concentration in the ash approximately 357 times, with its specific activity ranging from 0.16 to 3.4 kBq/g.

When burning one kg of forest litter (morphological layers A, B, and C), approximately 29 g, 48 g, and 192 g of ash were produced. This resulted in a corresponding $^{90}$Sr specific activity approximately 35, 21, and 5 times higher than the input material; the specific activity in the respective layers A, B, and C ash was 0.63, 0.92, and 3.3 kBq/g.

According to the data, 12 to 33% of the $^{90}$Sr activity in wood ash is washed out with water, and 10.8 to 13.2% of the $^{90}$Sr activity in forest litter ash is washed out.

Experiments unveiled that $^{90}$Y leaching is invisible, unlike the studied $^{90}$Sr leaching.

The leaching of $^{137}$Cs from wood ash with water was $89 \pm 4\%$, and from the ash of forest litter, corresponding to morphological layers A, B, and C, was $35.0 \pm 2.5\%$, $7.5 \pm 1.5\%$, and $1.1 \pm 0.5\%$, respectively.

Recently, researchers observed an increase in the specific activity of $^{90}$Sr in the water of observation wells drilled at the Chornobyl NPP, located downstream of the groundwater flow from the fire centers and within them. This increase varied from 2 to 60 times, reaching values of 180 Bq/l, which can be attributed to the local impact of recent fires.

The time interval between the significant 2020 fire and the appearance of elevated $^{90}$Sr concentrations in groundwater samples from observation wells was 2.7 years, a crucial period that does not contradict the results of predictions of $^{90}$Sr migration in the aeration zone under similar conditions[23].
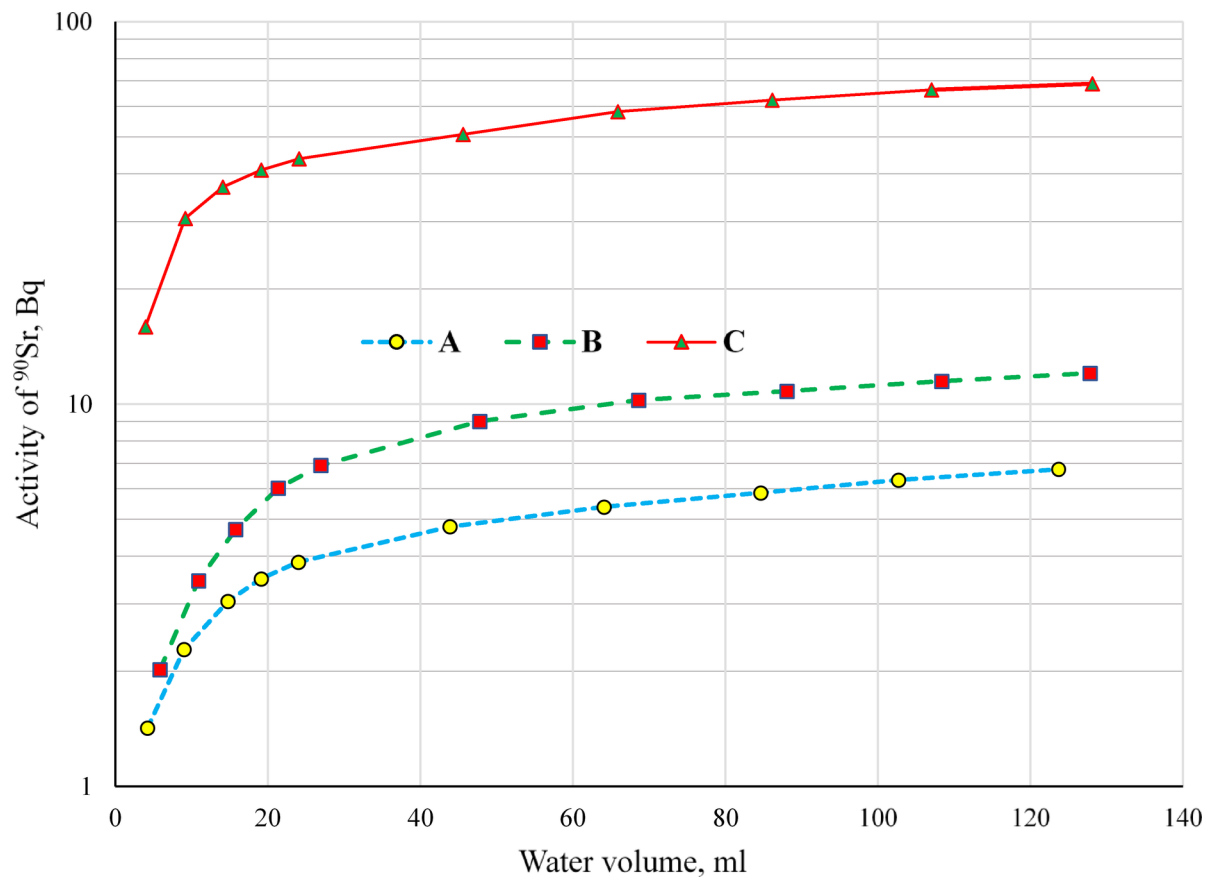
**Fig. 5**. Cumulative $^{90}$Sr activity leached from a forest litter ash sample with water, Bq.

The estimates obtained during the laboratory experiment indicate that fires in radionuclide-contaminated territories should be considered a notable source of $^{90}$Sr entering surface and groundwater. This requires appropriate amendments to the regulations for the radioecological monitoring of waters.
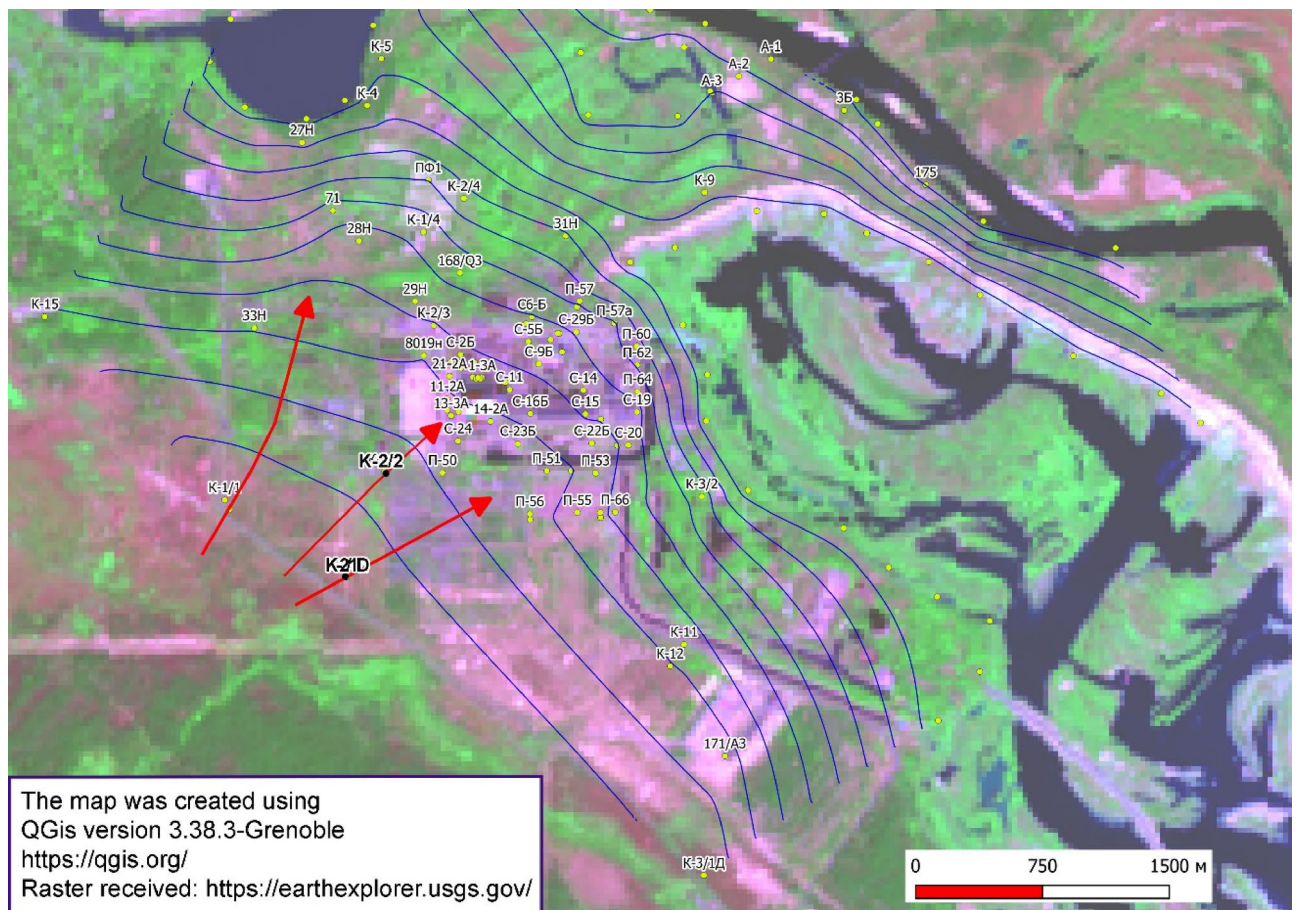
**Fig. 6**. Direction of the spread of contaminated groundwater from fires in 2020 in the "Red Forest" PTLRW area on the Landsat satellite image dated September 20, 2020.
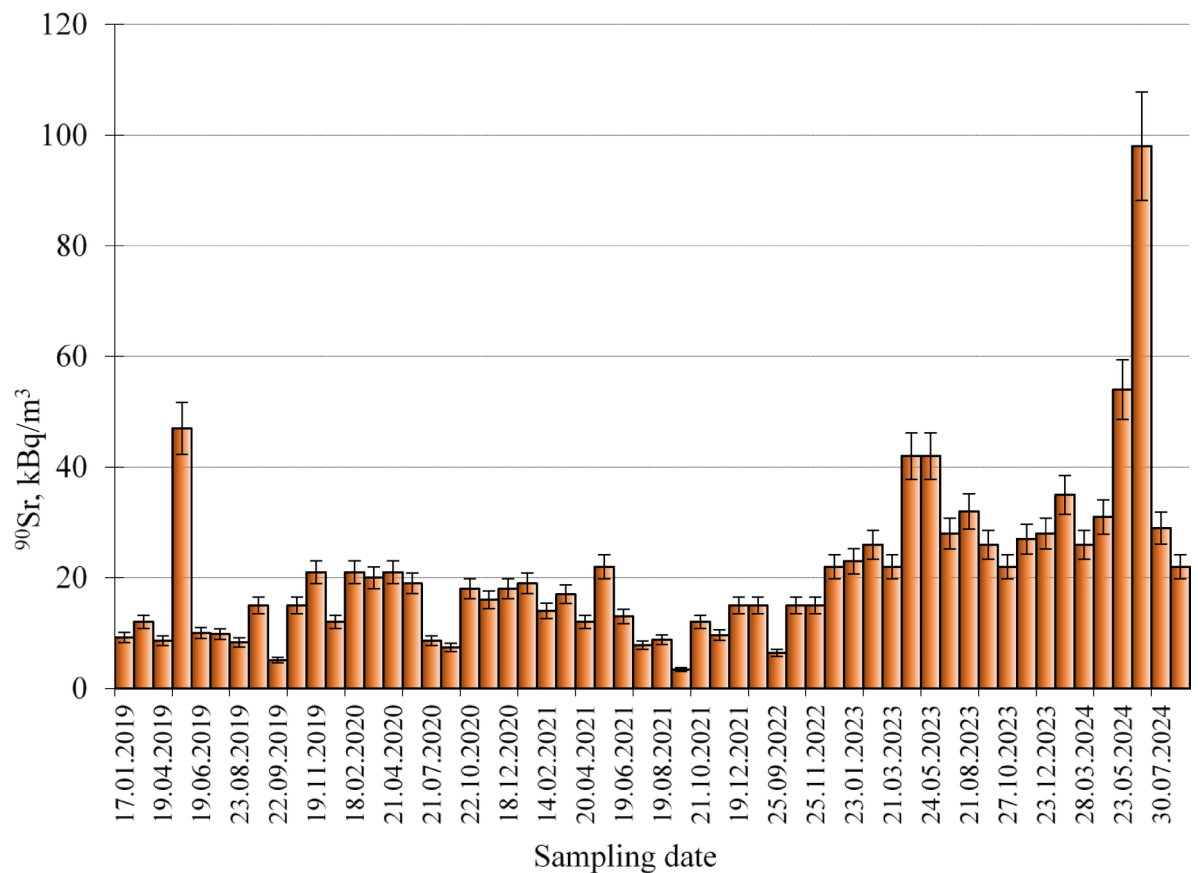
**Fig. 7**. Dynamics of change in specific activity of $^{90}$Sr in drilled well K-2/1, located downstream of groundwater flow from the burn site in 2020[25].
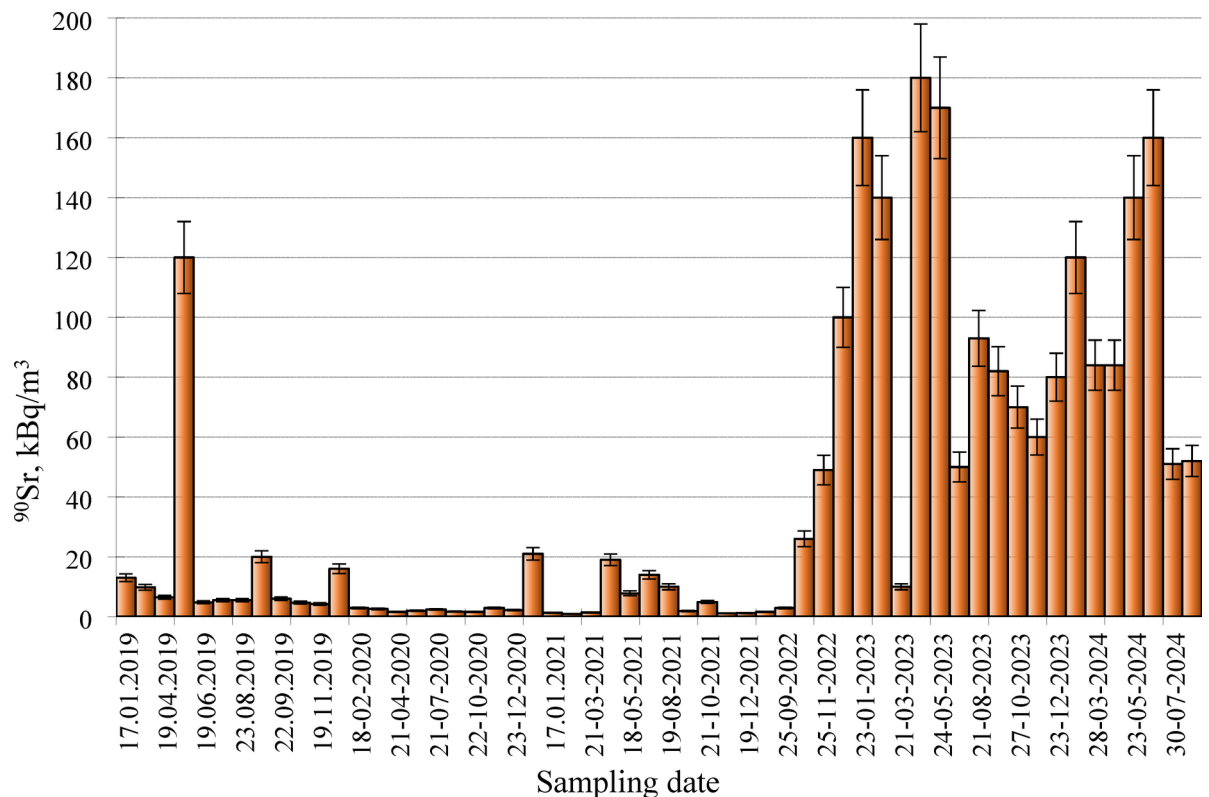
**Fig. 8**. Dynamics of change in specific activity of ^{90}Sr in drilled well K-2/2, located downstream of groundwater flow from the burn site in 2020[25].

## Data availability
All data generated or analysed during this study are included in this published article [and its supplementary information files].

## References
1. Kicińska, A. & Caba, G. Strontium leaching from municipal waste subjected to incineration. *Environ. Geochem. Health*. **46**, 220. https://doi.org/10.1007/s10653-024-01998-1 (2024).
2. Bodí, M. B., Mataix-Solera, J., Doerr, S. H. & Cerdà, A. The wettability of Ash from burned vegetation and its relationship to mediterranean plant species type, burn severity and total organic carbon content. *Geoderma* **160**, 599–607. https://doi.org/10.1016/j.geoderma.2010.11.009 (2011).
3. Sánchez-García, C. et al. Chemical characteristics of wildfire Ash across the Globe and their environmental and socioeconomic implications. *Environ. Int.* **178**, 108065. https://doi.org/10.1016/j.envint.2023.108065 (2023).
4. Pereira, P. et al. Wildfire effects on extractable elements in Ash from a *Pinus pinaster* forest in Portugal. *Hydrol. Process.* **28**, 3681–3690. https://doi.org/10.1002/hyp.9907 (2014).
5. Earl, S. R. & Blinn, D. W. Effects of wildfire Ash on water chemistry and biota in South-Western U.S.A. Streams. *Freshw. Biol.* **48**, 1015–1030. https://doi.org/10.1046/j.1365-2427.2003.01066.x (2003).
6. Kovalenko, I. O. et al. Factors influencing the increased ^{90}Sr radioisotope migration in highly alkaline groundwater at chornobyl NPP site. *J. Environ. Radioact.* **275**, 107431. https://doi.org/10.1016/j.jenvrad.2024.107431 (2024).
7. Bruchertseifer, F., Steiner, M., Hiersche, L., Savkin, B. & Poppitz-Spuhler, A. Wirth, E. Dynamics of strontium-90 in forest ecosystems. *Radioprotection* **37** (Cl), 409–413. https://doi.org/10.1051/radiopro/2002077 (2002).
8. Buzinny, M., Los, I. & Shepelevich, K. The distribution of ^{137}Cs and ^{90}Sr in the biomass of pine trees planted in 1987–1988 in the near zone of the Chernobyl nuclear power plant. *Appl. Radiat. Isot.* **52** (4), 905–910. https://doi.org/10.1016/S0969-8043(99)00142-6 (2000).
9. Holiaka, D. M., Levchuk, S. E., Yoschenko, V. I., Yoschenko, L. V. & Holiaka, M. A. The model of biogenic fluxes and depots of ^{90}Sr in contaminated pine stands. *Sci. Bull. Ukrainian Natl. Forestry Univ.* **29** (9), 81–86. https://doi.org/10.36930/40290914 (2019).
10. Yoschenko, V. et al. Long-term changes in ^{90}Sr pools of Scots pine biomass in the chornobyl red forest. *J. Environ. Radioact.* **273**, 107366. https://doi.org/10.1016/j.jenvrad.2023.107366 (2024).
11. Hu, J. et al. Application of a tuning-free burned area detection algorithm to the chornobyl wildfires in 2022. *Sci. Rep.* **13**, 5236. https://doi.org/10.1038/s41598-023-32300-5 (2023).
12. Hu, J. et al. Tuning-free moderate-scale burned area detection algorithm a case study in Chornobyl-contaminated region. *Int. J. Remote Sens.* **45**, 2444–2461. https://doi.org/10.1080/01431161.2024.2331976 (2024).
13. Igarashi, Y. et al. Effects of large-scale wildfires on the redistribution of radionuclides in the Chornobyl river system. *Environmental Science & Technology*. 58, 20630–20641. https://doi.org/10.1021/acs.est.4c07019 (2024).

14. Hygienic requirements for drinking water intended for human consumption: state health and safety standards and rules DSanPiN 2.2.4-171-10, Kyiv, 2010. https://zakon.rada.gov.ua/laws/show/z0452-10#Text (2010).
15. Buzinny, M., Likhtarev, I., Los, I., Talerko, N. & Tsigankov N. [14]C analysis of annual tree rings from the vicinity of the Chernobyl NPP. *Radiocarbon* **40** (1), 373–379. https://doi.org/10.1017/S0033822200018257 (1997).
16. Buzinny, M. Radioactive graphite dispersion in the environment in the vicinity of the Chernobyl nuclear power plant. *Radiocarbon* **48** (3), 451–458. https://doi.org/10.1017/S003382220003887X (2006).
17. Buzynnyi, M., Romanenko, O., Mykhailova, L., Lytvynko, A. & Panasiuk, M. Traces of ^{14}C emissions for the operation period of two Ukrainian NPPS: Rivne and chornobyl. *Radiocarbon* **65** (2), 335–342. https://doi.org/10.1017/RDC.2023.3 (2023).
18. Levchuk, S. Handbook of basic methods for determining the activity of radionuclides. National University of Life and Environmental Sciences of Ukraine, Kyiv, 2016. http://uiar.org.ua/Dovidnyk.pdf Google Scholar: https://scholar.google.com.ua/scholar?hl=en&as_sdt=0,5&cluster=17236881149847303149 (2016).
19. Amiro, B. D., Sheppard, S. C., Johnston, F. L., Evenden, W. G. & Harris, D. R. Burning radionuclide question: what happens to iodine, cesium and Chlorine in biomass fires? *Sci. Total Environ.* **187** (2), 93–103. https://doi.org/10.1016/0048-9697(96)05125-X (1996).
20. Shynkarenko, V. K. & Novikov, A. M. Air releases of ^{137}Cs from the burning of contaminated biomass: a review of laboratory research. *Nuclear Power and the Environment.* 3(31), 69–78. https://doi.org/10.31717/2311-8253.24.3.7 (2024).
21. Buzynnyi, M. Practical aspects of the application of Cherenkov counting method with the correction of sample's color quenching. *Environment & Health.* 2(107), 40–46. doi:10.32402/dovkil2023.02.040 (2023).
22. Beta spectrometer SEB-01. Operation manual. Research and Production Enterprise ATOM KOMPLEX PRYLAD. A.A. Balkema Publisher. http://www.akp.com.ua/index.php?option=com_content&view=article&id=119&Itemid=106 (2002).
23. Dzhepo, S.P., Skal'skii, A. S. Radioactive contamination of groundwater within the Chernobyl exclusion zone in *Chernobyl Disaster and Groundwater* (ed. Shestopalov, V.) 25–71 https://books.google.com.ua/books?id=MUl16_H8MksC (2002).
24. Starikov, N. B., Alfyorov, A. M., Panasyuk, M. I., Lytvyn, I. A. & Liushnya, E. P. Simulation of migration of radionuclides in the zone of aeration at the industrial site of the Ukryttya object. *Saf. Issues Nuclear Power Plants Chernobyl.* **18**, 96–102 (2012). http://dspace.nbuv.gov.ua/handle/123456789/113337
25. Monthly reports on the radiation state of the exclusion zone environment. *State Specialized Enterp. Ecocentre (Period* (2024). 17.01.2019–30.07.2024).

## Acknowledgements

## Author contributions

MP - idea, curation of research, writing the manuscript; MB - experimental research, LSC measurements, data curation, preparing and writing the manuscript; SK- presenting data on 90Sr in water, discussing results and the manuscript; NS- discussion results, preparing Fig. 6 and a draft of the manuscript; IK- discussion results and a draft of the manuscript; LM- gamma-spectroscopy research, discussing results and the manuscript.

## Declarations

## Competing interests

The authors declare no competing interests.

## Additional information

**Correspondence** and requests for materials should be addressed to M.B.

**Reprints and permissions information** is available at www.nature.com/reprints.

**Publisher's note** Springer Nature remains neutral with regard to jurisdictional claims in published maps and institutional affiliations.